# An investigation of the influence of two-stage drying conditions on convective drying of porous materials

K. Murugesan, H.R. Thomas and P.J. Cleall
*Geoenvironmental Research Centre, Cardiff School of Engineering, Cardiff University, Cardiff, UK*

Received July 2001
Revised August 2001
Accepted September 2001

***Keywords*** *Porous media, Drying*

***Abstract*** *A numerical study is carried out to investigate the influence of multistage drying regimes on the drying kinematics of a porous material. In particular the effects of varying the conditions of the drying medium are studied. The drying model for the solid is developed based on the continuum approach. A series of simulations of the drying behaviour of a rectangular brick with varying temperature, heat transfer coefficient and relative humidity of the drying medium are undertaken. It is found that the total drying time is mainly dependent on the relative humidity of the drying medium. Also condensation is predicted on the surface of the brick, with the quantity of condensation being directly linked to the relative humidity and temperature of the drying medium. Overall it is concluded that multistage drying regimes are useful in reducing the overall drying time whilst avoiding detrimental shrinkage during the constant drying period.*

## Nomenclature

$C$ = specific heat capacity (J/kg K)
$C^*$ = equivalent specific heat (J/kg K)
$D$ = diffusion coefficient
$D_m$ = isothermal diffusion coefficient ($m^2$/s)
$D_T$ = non-isothermal diffusion coefficient ($m^2$ sK)
$H$ = enthalpy (J/kg K)
$h_c$ = convective heat transfer coefficient (W/$m^2$ K)
$h_m$ = convective mass transfer coefficient (m/s)
$J$ = mass flux (kg/$m^2$s)
$k$ = thermal conductivity (W/mK)
$M$ = mass (kg)
$m$ = rate of phase change (kg/s)
$t$ = time (s)
$T$ = temperature (K)
$w$ = moisture content in liquid or vapour phase (kg/kg of dry solid)
$W$ = total moisture content ($w_l$+$w_v$)
$x$,$y$ = spatial coordinates

Greek symbols

$\pi$ = relative humidity
$\rho$ = density (kg/$m^3$)

Subscripts

$i$ = node of an element
$j$ = mobile component (liquid or vapour); node of an element
$k$ = node of an element
$l$ = liquid
$s$ = surface conditions
$v$ = vapour
$w$ = moisture (liquid or vapour)
$\propto$ = ambient conditions

The first author gratefully acknowledges the financial contribution of the Geoenvironmental Research Centre, which enabled him to visit Cardiff. Also, thanks are expressed to the Department of Mechanical Engineering, KREC, for releasing him for this period of time.

International Journal of Numerical Methods for Heat & Fluid Flow, Vol. 12 No. 1, 2002, pp. 29–46.

DOI 10.1108/09615530210413154

## Introduction

The binder removal process in tile and brick industries is very important as excess moisture has to be removed from products, which are already in their final shape. This process demands utmost care so that the geometry and size of the products are not affected. The safest way is to remove the excess moisture in evaporative drying conditions. However, this is a time consuming process, which also has to depend on the ambient conditions. One possible solution is to dry the solids via a multistage process (Hawlader *et al.*, 1997). The products can be dried in an evaporative atmosphere until the constant drying period, during which maximum shrinkage of the products takes place (Kowalski *et al.*, 1997). Beyond this point they can be dried using air at a relatively higher temperature in order to reduce the total drying time.

Drying is a complex phenomenon that involves simultaneous heat and mass transfer to and from the solid. Drying behaviour can be understood with the help of mathematical models. The drying of a solid is affected by both internal and external resistance for heat and mass transfer (Ford, 1986). The internal mechanism of moisture transfer can be due to capillary forces during the constant rate drying period or due to diffusion during the falling rate period Luikov, 1996). These different regimes of drying have been studied theoretically with the help of one-dimensional (Huang, 1979; Kallel *et al.*, 1993) and two-dimensional (Comini and Lewis, 1976; Ferguson and Lewis, 1991) models. The external resistance for heat and mass transfer is affected by the temperature, convective heat and mass transfer coefficient and relative humidity of the drying medium. Normally the heat and mass transfer coefficient values are obtained from simple boundary layer correlation or from conjugate analysis (Oliveira and Haghighi, 1995).

The internal mechanism of moisture transport is modelled using different approaches. Van der Zanden and Schoenmakers (1996) represented the simultaneous transport of liquid and vapour in terms of concentration of the respective phases. Evaporation inside the porous material was taken into account with a mass transfer coefficient. They obtained drying results for clays of different hygroscopicity. They found that the moisture profiles inside the clay are not greatly influenced by whether the flux at the surface is due to vapour or liquid transfer. They suggest that more study concerning the physics at the drying surface is required. Fyhr and Rasmuson (1997) developed a two-dimensional model for drying of softwoods like pine and spruce. The flow of water, air and vapour inside the solid was represented by an extended Darcy's law. The diffusion of bound water was modelled via Fick's law. They considered heat transfer within the solid both by conduction and convection. They found that drying is controlled by internal mass transfer during the main part of the drying process. A semi-analytical model with an assumption of a drying front has been developed by Perre *et al.* (1999) to study the drying behaviour of sapwood and heartwood. They assumed that the porous medium

was divided into two zones, a vapour zone and a liquid zone. The water vapour was assumed to migrate only according to Darcy's law, neglecting diffusion processes. They found the duration of the constant drying rate was directly connected to the liquid migration, whose value depended on both the drying flux and on the liquid migration coefficient.

Kowalski *et al.* (1997) developed a two-dimensional drying model based on the thermomechanical concept proposed by the authors in their previous works. They studied the response of a clay bar when exposed to a drying medium of varying temperature and humidity. They also calculated the drying induced stresses using an elastic model. The above studies were carried out for the constant drying rate period of the material. They found that the response of the material to the alteration of moisture was almost instantaneous, whereas for temperature, the material was subject to some retardation. Dietl *et al.* (1998) developed a model based on heat and enthalpy as well as mass balance in the liquid and vapour phases for a differential control volume. They determined the moisture conductivity and vapour diffusion resistance required for their model by an inversion procedure, using experimentally obtained drying curves for concrete and pine. They tested their model for time dependent drying conditions that are required in packed bed drying.

Although a number of investigations have been carried out with respect to the aspect of internal moisture transport of porous materials during drying, there is little work available on the effect of external resistances, i.e. the heat transfer coefficient, temperature and relative humidity of the drying medium on the drying behaviour of the solid. Also Nasrallah and Perre (1988) suggested that a study on the influence of heat transfer coefficients on drying was needed. Within the context of a study of multistage drying, this paper will focus on these particular aspects.

In this study, trials have been made to investigate the drying of a rectangular brick of size $0.2 \times 0.1$ m. The effect of variation in temperature (313, 333 and 353 K), relative humidity (30, 50 and 70 per cent) and heat transfer coefficient (15 and 30 $W/m^2$ K) of the drying medium, on the drying behaviour of the brick is studied via numerical simulation. The numerical model has been developed based on the continuum approach and is discussed in the following section.

## Mathematical model and numerical solution procedure

The governing equations for the porous solid are obtained using a continuum approach (Huang, 1979; Murugesan *et al.*, 2000). The densities of the solid matrix, liquid and gaseous phases are assumed to be constant. The viscous dissipation and convective terms are neglected in the energy equation. It is also assumed that there exists local thermal equilibrium between the solid matrix, pure liquid and gaseous mixture of air and vapour.

*Governing equations*

The two-dimensional conservation equations for liquid and vapour in porous solid can be obtained using species equations (Huang, 1979). In the specific case under consideration here, namely two stage drying regimes, internal heat and moisture movement are focussed upon. A set of two coupled governing differential equations for the thermal and moisture fields are described here following the approach presented previously by the first two authors and co-workers (Murugesan *et al.*, 2000). Since the problem under consideration here focuses on drying alone, in the absence of shrinkage effects, the formulation is restricted in this presentation to those aspects alone (Murugesan *et al.*, 2000).

Liquid

$$\frac{\partial w_l}{\partial t} = -\frac{1}{\rho_o}\left[\frac{\partial J_{lx}}{\partial x} + \frac{\partial J_{ly}}{\partial y}\right] + \frac{m}{M_o} \tag{1}$$

Vapour

$$\frac{\partial w_v}{\partial t} = -\frac{1}{\rho_o}\left[\frac{\partial J_{vx}}{\partial x} + \frac{\partial J_{vy}}{\partial y}\right] - \frac{m}{M_o} \tag{2}$$

where $J$ is the diffusion flux of moisture and $w$ is the moisture content per kg of dry solid.

The energy equation for the porous solid is

$$\rho_o \frac{\partial}{\partial t}\left(\sum w_j H_j\right) = \frac{\partial}{\partial x}\left(k\frac{\partial T}{\partial x}\right) + \frac{\partial}{\partial y}\left(k\frac{\partial T}{\partial y}\right) - \frac{\partial}{\partial x}\left(\sum J_j H_j\right) - \frac{\partial}{\partial y}\left(\sum J H_j\right) \tag{3}$$

where $j$ represents liquid or vapour.

Liquid movement during the earlier part of drying can be represented using Darcy's law and the diffusion of vapour during the falling rate period can be represented using Fick's law. Using the above two laws, Equations (1) and (2) can be represented in terms of moisture and temperature gradients, multiplied by transport coefficients. These transport coefficients are functions of moisture content and temperature. Hence the final form of equations (1) and (2) can be written as follows:

$$\frac{\partial w_l}{\partial t} = \frac{\partial}{\partial x}\left[D_{ml}\frac{\partial W}{\partial x} + D_{Tl}\frac{\partial T}{\partial x}\right] + \frac{\partial}{\partial y}\left[D_{ml}\frac{\partial W}{\partial y} + D_{Tl}\frac{\partial T}{\partial y}\right] + \frac{m}{M_o} \tag{4}$$

$$\frac{\partial w_v}{\partial t} = \frac{\partial}{\partial x}\left[D_{mv}\frac{\partial W}{\partial x} + D_{Tv}\frac{\partial T}{\partial x}\right] + \frac{\partial}{\partial y}\left[D_{mv}\frac{\partial W}{\partial y} + D_{Tv}\frac{\partial T}{\partial y}\right] - \frac{m}{M_o} \tag{5}$$

where $D_{ml}$, $D_{Tl}$, $D_{mv}$, $D_{Tv}$ represent isothermal and non-isothermal transport coefficients.

The rate of condensation can be obtained from equations (4) and (5) as follows:

$$\frac{m}{M_o} = \frac{\partial}{\partial x}\left[D_{mv}\frac{\partial w_l}{\partial x} + D_{Tv}\frac{\partial T}{\partial x}\right] + \frac{\partial}{\partial y}\left[D_{mv}\frac{\partial w_l}{\partial y} + D_{Tv}\frac{\partial T}{\partial y}\right] \tag{6}$$

Compared to $w_l$, the value of $w_v$ can be neglected and hence the summation of equations (4) and (5) will give the final form of the moisture conservation equation for the porous solid, representing the liquid and transport during the different regimes of drying.

The final form of the moisture conservation equation is

$$\frac{\partial W}{\partial t} = \frac{\partial}{\partial x}\left[(D_{mv} + D_{ml})\frac{\partial W}{\partial x} + (D_{Tv} + D_{Tl})\frac{\partial T}{\partial x}\right] + \frac{\partial}{\partial y}\left[(D_{mv} + D_{ml})\frac{\partial W}{\partial y} + (D_{Tv} + D_{Tl})\frac{\partial T}{\partial y}\right] \tag{7}$$

The convective term in the energy equation is very small compared to the diffusion equation (Kallel *et al.*, 1993). Hence by dropping the convective term in the energy equation (3), the final form of the energy equation for the porous solid can be written as follows:

$$C^*\frac{\partial T}{\partial t} = \frac{1}{\rho_o}\left[\frac{\partial}{\partial x}\left(k\frac{\partial T}{\partial x}\right) + \frac{\partial}{\partial y}\left(k\frac{\partial T}{\partial y}\right)\right] + \frac{m}{M_o}(H_v - H_l) \tag{8}$$

where the equivalent specific heat capacity of the porous solid is determined as

$$C* = C_o + w_l C_l + w_v C_v$$

Equations (7) and (8) are the final forms of the mass and energy transport equations for the porous solid.

*Boundary conditions*

The porous solid (brick) is dried by convective drying on all the sides, except the bottom side, where an adiabatic boundary condition for both heat and mass transfer is assumed.

The convective boundary condition for mass transfer is

$$D_{mv}\frac{\partial W}{\partial n} + D_{Tv}\frac{\partial T}{\partial n} = h_m(\rho_s - \rho_\infty) \tag{9}$$

The convective boundary condition for heat transfer is

$$k\frac{\partial T}{\partial n} + \rho_o(H_v - H_l)\left(D_{Tv}\frac{\partial T}{\partial n} + D_{mv}\frac{\partial W}{\partial n}\right) = h_c(T_\infty - T_s) + (H_v - H_l)h_m\left(\rho_s - \rho_\infty\right) \quad (10)$$

*Numerical solution procedure*

The Galerkin weighted residual method has been used to integrate governing equations (7) and (8). The variables in the equations are represented by means of linear triangular elements. Within each element, the temperature $T$ and moisture content $W$ are represented in terms of their nodal values using the following expressions:

$$T = N_i T_i + N_j T_j + N_k T_k$$

$$W = N_i W_i + N_j W_j + N_k W_k$$

where $N_i$, $N_j$ and $N_k$ are the nodal shape functions.

The time derivatives in equations (7) and (8) are discretized using a forward finite difference method. A program has been developed to compute the variation of temperature and moisture content at every time step until the solid reaches its equilibrium moisture content.

*Validation*

The drying model has been validated against the experimental results of Kallel *et al.* (1993) for the one dimensional model. Details of this work are presented elsewhere Murugesan *et al.*, 1996). The two dimensional model has been used in the conjugate drying analysis of a rectangular brick. The temperature and moisture contours predicted using this model have been compared with the conjugate results of Oliveira and Haghighi (1995) and are shown in Figures 1 and 2. Our results show qualitative agreement with those of Oliveira and Haghighi (1995). The differences observed are due to the transport coefficients required for the model not being available for wood.

## Simulations

The drying of a rectangular brick of size $0.2 \times 0.1$ m is considered. The brick is assumed to have an initial temperature of 293 K and moisture content of 0.13 kg/kg of dry solid. For the first stage of drying the brick is dried in evaporative drying conditions, i.e. using air at 293 K with 50 per cent relative humidity. The brick is then further dried, in the second drying stage, using air with different values of temperature, heat transfer coefficient, mass transfer coefficient and relative humidity. The solid is said to be dried when it reaches

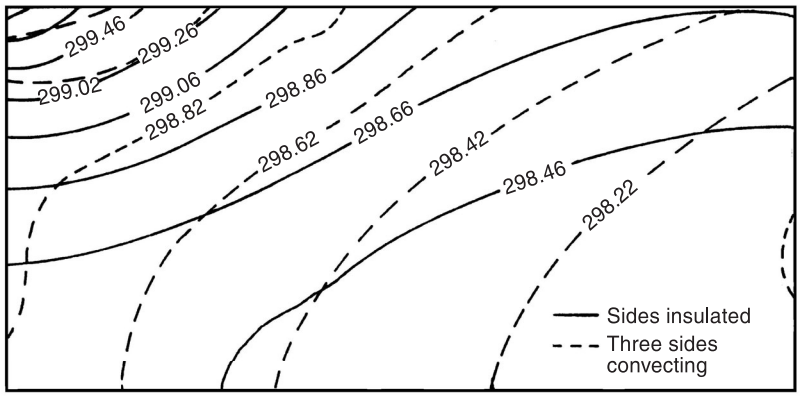


**Figure 1.**
Comparison of temperature contours at 2 h for timber drying analysis at Re = 200

**Note:** Ti = 298.0 K, $T_{\infty}$ = 333.0 K, Wi = 0.45, $\phi$ = 10%

its equilibrium moisture content, (0.005 kg/kg of dry solid in the present case). Assuming the heat and mass transfer analogy throughout the drying period, the ratio between the convective heat transfer coefficient $h_c$ and the connective mass transfer coefficient $h_m$, is taken as 1000. The temperatures of air considered are 313, 333 and 353 K. Three values of relative humidity are considered—30, 50 and 70 per cent. The heat transfer coefficients used are 15 and 30 W/m$^2$K. Table I shows a matrix of the second stage drying conditions for the 18 simulations undertaken.

The drying program was run to represent a maximum of 400 h, at which time the brick had reached its equilibrium moisture content in each case. In all the 18 drying trials, the brick initially underwent a first drying stage with drying conditions using air at a temperature of 293 K and 50% relative

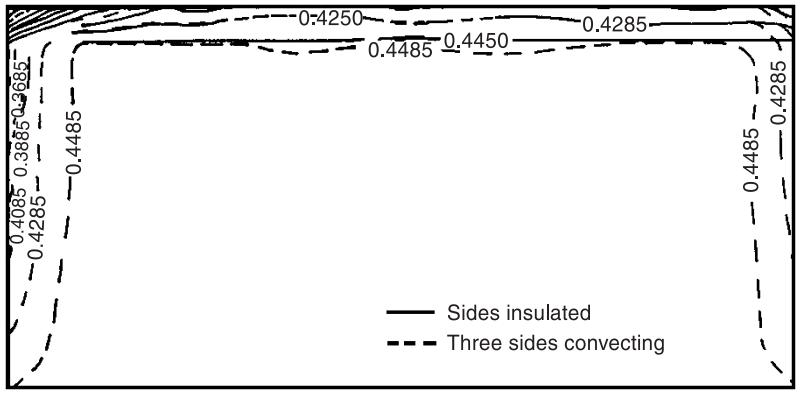


**Figure 2.**
Comparison of moisture contours at 2 h for timber drying.

| Simulation number | Relative humidity, $\vartheta$ | Temperature, $T$ (K) | Heat transfer coefficient, $h_c$ (W/m$^2$K) |
|---|---|---|---|
| 1 | 30 | 313 | 15 |
| 2 | | | 30 |
| 3 | | 333 | 15 |
| 4 | | | 30 |
| 5 | | 353 | 15 |
| 6 | | | 30 |
| 7 | 50 | 313 | 15 |
| 8 | | | 30 |
| 9 | | 333 | 15 |
| 10 | | | 30 |
| 11 | | 353 | 15 |
| 12 | | | 30 |
| 13 | 70 | 313 | 15 |
| 14 | | | 30 |
| 15 | | 333 | 15 |
| 16 | | | 30 |
| 17 | | 353 | 15 |
| 18 | | | 30 |

**Table I.**
Second stage drying conditions

humidity for 10 h. The various second stage drying conditions were then applied.

*Discussion of results*

The results obtained are represented in the form of rate of drying curves, time evolutions of average moisture content of the solid and temperature and moisture evolutions at the surface of the brick (i.e. at $x = 0.0$ and $y = 0.05$ m). The results obtained from the 18 drying trials are presented in the form of various plots to describe the response of the solid when subjected to different second stage drying conditions. Each figure represents the variation of a particular drying parameter (i.e. three temperatures of air, 313, 333 and 353 K and two values of heat transfer coefficient, 15 and 30 W/m$^2$K) for a fixed value of relative humidity. Hence in every figure there are six curves showing the effects of the variation of the temperature and heat transfer coefficients.

*Rate of drying*. The variation of the rate of drying with time is shown in Figures 3–5 for relative humidity values of 30, 50 and 70 per cent respectively. Even though results are obtained for 400 h of drying, the results are shown up to 15 h only because significant changes in the rate of drying are observed only during this period. The transfer of moisture between the solid surface and drying medium takes place due to the concentration difference between the surface of the solid and the drying medium.

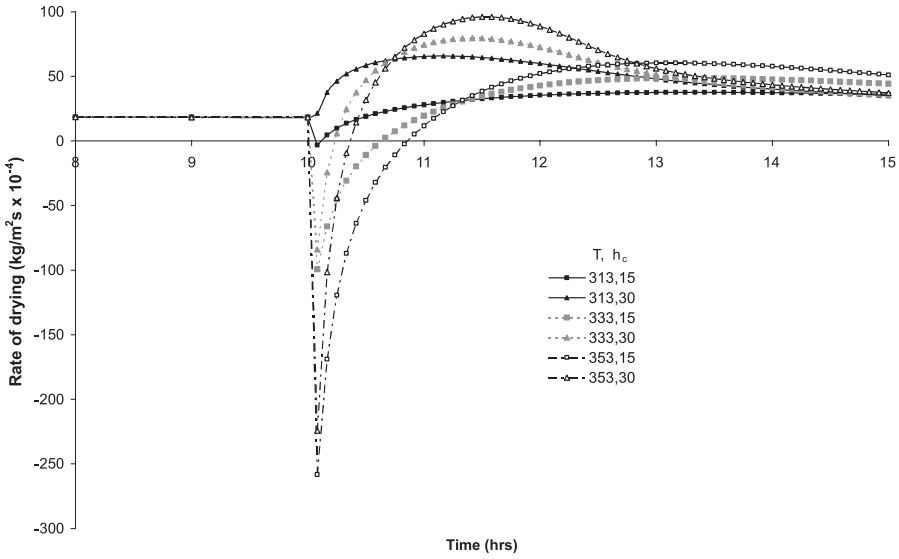


**Figure 3.**
Effect of $T$ and $h_c$ on rate of drying for $\phi$ = 30 per cent

For each of the 18 drying trials the first stage of drying is the same. During this first stage, there is a reduction in the temperature of the solid during the initial drying period. The solid reaches the wet bulb temperature (286.5 K) corresponding to the initial drying conditions (293 K and 50% relative humidity). During the first 3 h of this stage the drying rate increases, the rate then remains constant until the end of the stage (10 h).

When the solid is dried in the second stage using air at higher temperatures and at higher values of relative humidity, condensation may occur. This condensation of water vapour from the drying medium onto the solid occurs when the vapour concentration in the air is higher than that at the surface. This is indicated by the negative value of the drying rates seen in Figures 3–5. Such condensation can be observed for all of the second stage drying conditions with the exception of simulation 2 which has a relative humidity of 30%, a heat transfer coefficient of 30 W/m$^2$K and a temperature of 313 K. In comparison to simulation 2, in simulation 1, which has a lower value of heat transfer coefficient of (15 W/m$^2$K), a little condensation is observed, as shown in Figure 3. This is because in simulation 2 the solid tends to heat up more (see Figures 9–11), resulting in a higher concentration of water vapour at the solid surface.

For the regimes with higher air temperature, the humidity in the air increases for a fixed value of relative humidity. Hence for the higher temperatures (333 and 353 K), significant condensation is observed (Figure 3) from the very beginning of the second stage drying (i.e. after 10 h) as the humidity of the air is similarly increased by an elevated concentration of water vapour. In general, for higher temperatures and lower heat transfer coefficients

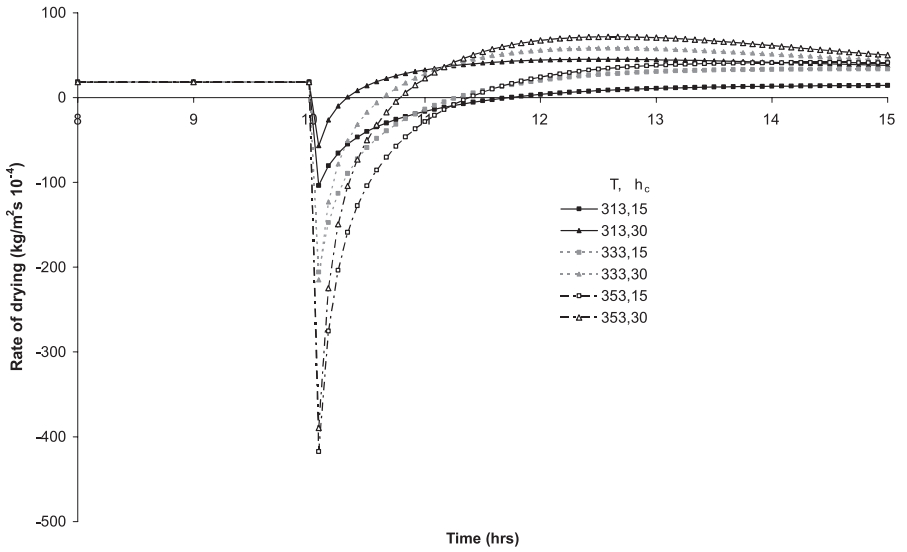


**Figure 4.**
Effect of $T$ and $h_c$ on rate of drying for $\phi$ = 50 per cent

more condensation is observed. Similar trends can be observed in Figures 4 and 5 with air at the highest temperature and highest heat transfer coefficient attaining the maximum drying rate during the initial drying, with the lowest drying rate during the falling rate period.

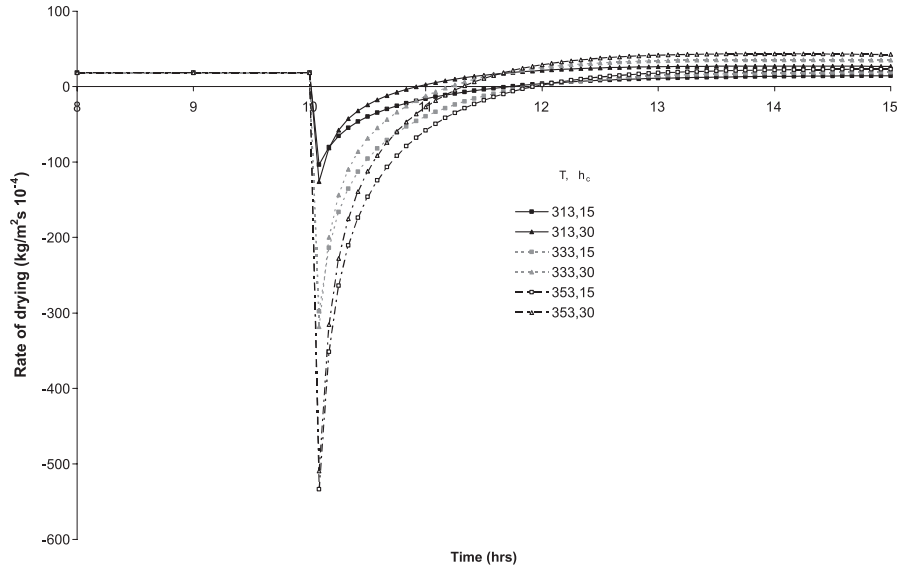


**Figure 5.**
Effect of $T$ and $h_c$ on rate of drying for $\phi$ = 70 per cent

When the relative humidity of air is increased, one expects more condensation to occur. This can be observed for all the cases shown in Figures 4 and 5. Again air with a higher temperature and a lower value of heat transfer coefficient gives rise to more condensation.

The values of temperature and heat transfer coefficient affect the condensation and drying behaviour of the solid only in the initial stages of the second drying stage. Beyond that the drying behaviour is driven by the relative humidity, with lower values leading to a higher rate of drying and therefore a lower total drying time. Perre *et al.* (1999) and Fyhr and Rasmuson (1997) have also observed these trends.

*Evolution of average moisture content with time*. The evolutions of average moisture content for each of the drying regimes are shown in Figures 6–8.

The effect of the condensation observed in the rate of drying curves can be clearly seen in these figures. Again at higher temperatures and higher relative humidity, an increase in the quantity of condensation can be observed.

The effect of condensation is observed only during the initial heating period of the second drying stage. After this, for the same value of heat transfer coefficient, the curves tend to the evolution associated with the lowest temperature of 313 K. The time taken to converge on this curve depends on the relative humidity and not on the temperature as can be observed in Figures 6–8. With an increase in relative humidity the time increases. Beyond this point of convergence, all of the tests behave in the same manner.

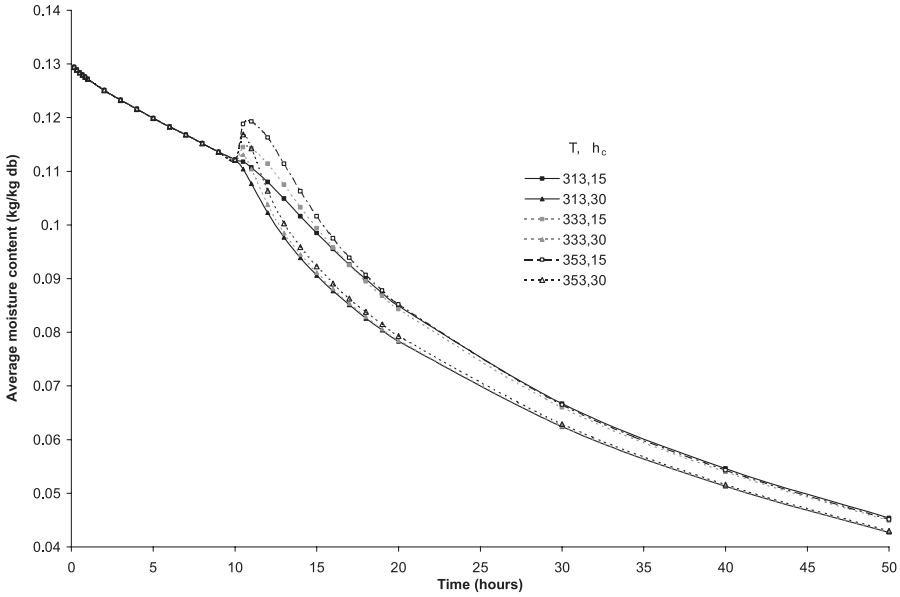


**Figure 6.**
Effect of $T$ and $h_c$ on evolution of average moisture content for $\phi$ = 30 per cent

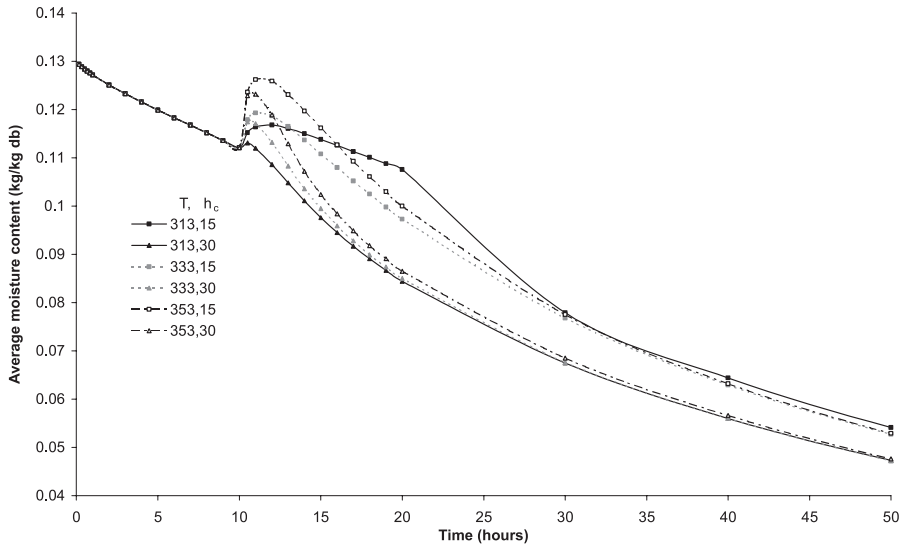


**Figure 7.**
Effect of $T$ and $h_c$ on evolution of average moisture content for $\phi$ = 50 per cent

When the relative humidity is equal to 30 per cent the drying potential, i.e. the difference between the vapour concentration at the solid surface and the drying medium, is greater than for the higher values of relative humidity. With an increase in the temperature of air, the humidity increases for a given relative humidity. Therefore, the maximum drying potential corresponds to the lowest temperature (313 K), resulting in a faster drying from the cooler air, as seen in Figure 6.

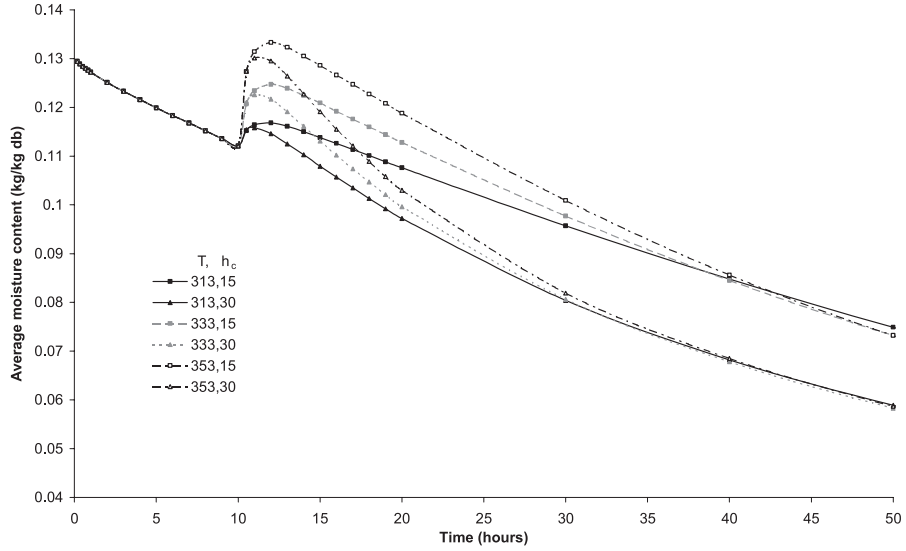


**Figure 8.**
Effect of $T$ and $h_c$ on evolution of average moisture content for $\phi$ = 70 per cent

Differences in drying behaviour are more clearly observed with higher relative humidity as seen in Figures 7 and 8. When the relative humidity is increased to 50 and 70 per cent the vapour concentration in air is initially higher than that at the surface of the solid. This results in condensation, as was observed in Figures 3–5. As expected with a higher temperature more condensation is observed. Air with higher values of heat transfer coefficient tends to dry the solid faster, as the solid heats up more rapidly and the quantity of condensation decreases owing to the rise in the concentration potential between the solid surface and air. The pattern of the internal moisture field followed, as would be expected, a trend of increasing moisture content towards the centre of the brick. This gradient of moisture content is a result of the drying at the surface of the brick described below in "Moisture evolutions with time at the surface", with the internal gradients being a function of the difference in moisture content at the surface and moisture content at the centre.

*Temperature evolutions with time at the surface*. The temperature evolutions at the surface of the brick are shown in Figures 9–11 for three different relative humidity values, 30, 50 and 70 per cent, respectively. After 10 h, the solid tends to heat up to the temperature of air. The rate of heating is higher with higher values of heat transfer coefficient.

The effect of the heat transfer coefficient on initial heating, say up to 30 h, is most significant at lower values of relative humidity. The time taken to reach the ambient temperature of air decreases with an increase in relative humidity. In all cases the solid reaches the temperature of the drying medium within 100 h.

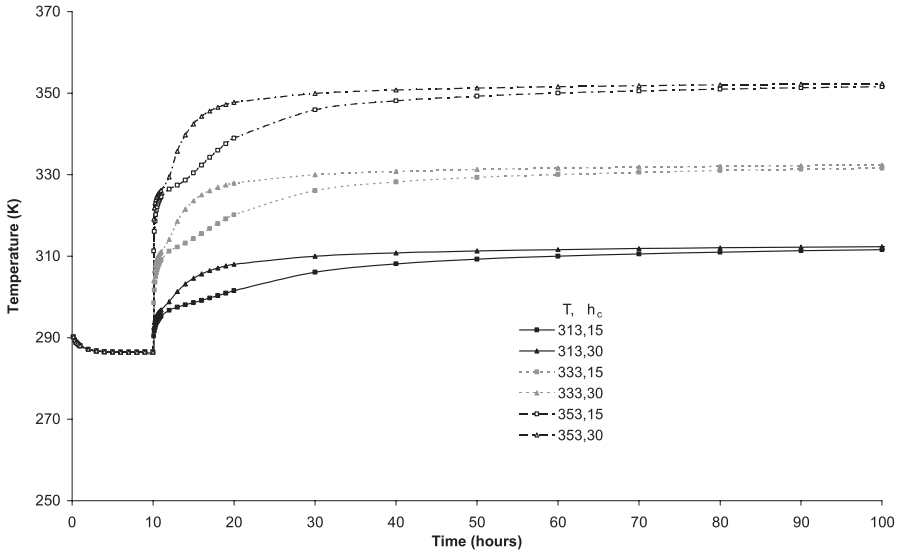


**Figure 9.**
Effect of $T$ and $h_c$ on evolution of temperature at surface for $\phi$ = 30 per cent

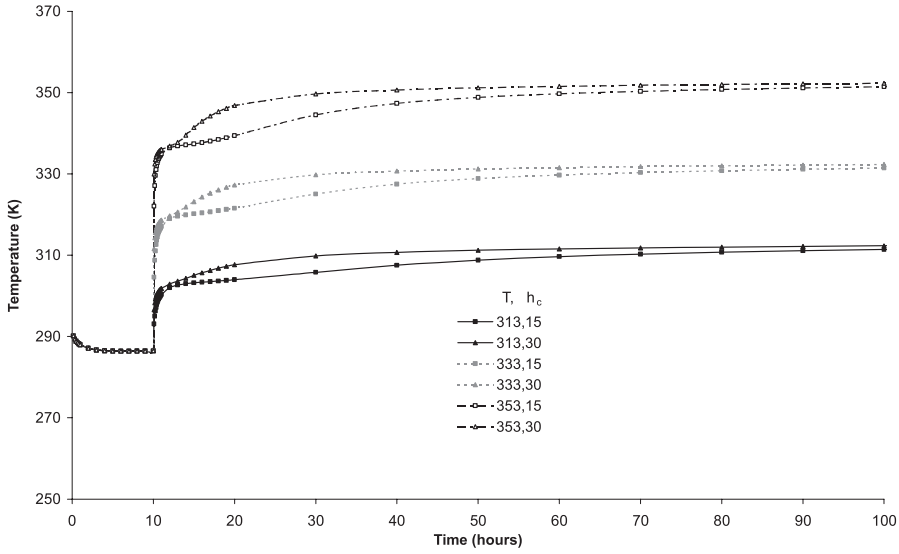


**Figure 10.**
Effect of $T$ and $h_c$ on evolution of temperature at surface for $\phi$ = 50 per cent

Overall, during drying the solid reaches thermal equilibrium much faster than moisture equilibrium. Also the time taken to achieve thermal equilibrium is directly related to temperature and inversely related to the heat transfer and relative humidity of the drying medium.

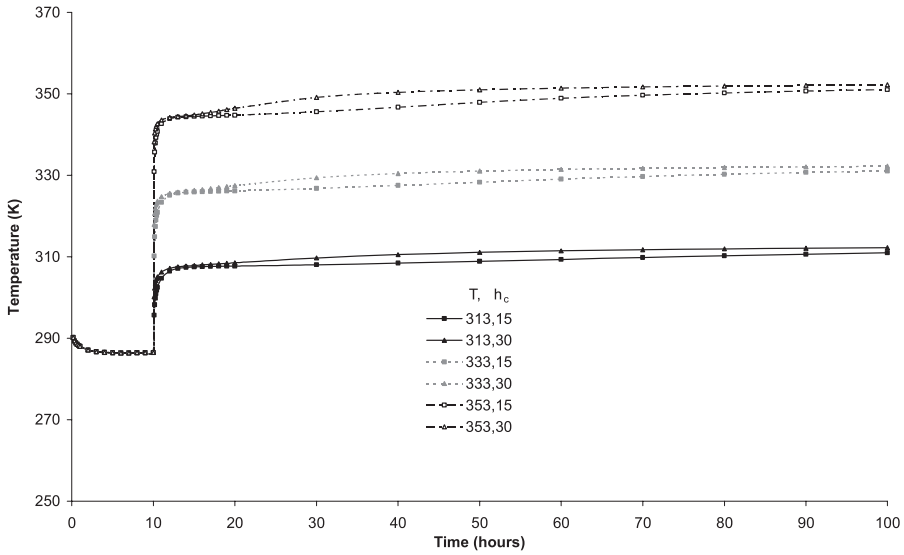


**Figure 11.**
Effect of $T$ and $h_c$ on evolution of temperature at surface for $\phi$ = 70 per cent

*Moisture evolutions with time at the surface*. The moisture evolutions at the brick surface are shown in Figures 12–14. As both drying and condensation take place at the surface of the brick, the effects of these processes are most clearly observed at the surface. From the figures it can be seen that the amount of condensation increases with higher ambient temperatures and relative humidity. Later the moisture content decreases at the surface due to drying and

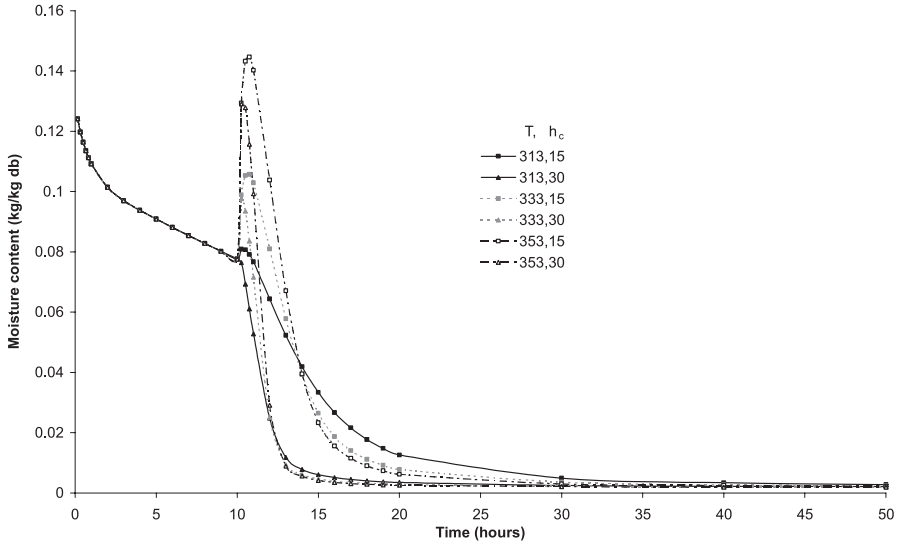


**Figure 12.**
Effect of $T$ and $h_c$ on evolution of moisture content at surface for $\phi$ = 30 per cent

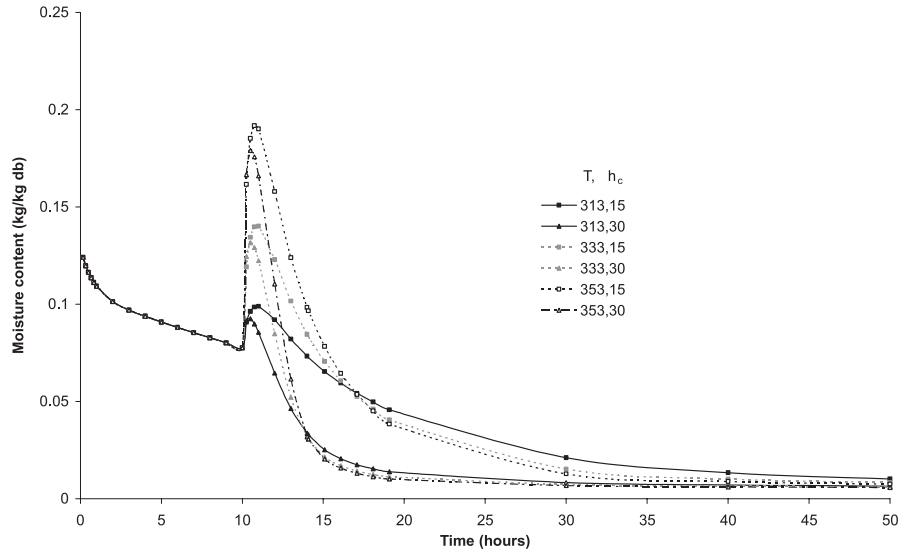


**Figure 13.**
Effect of $T$ and $h_c$ on evolution of moisture content at surface for $\phi$ = 50 per cent

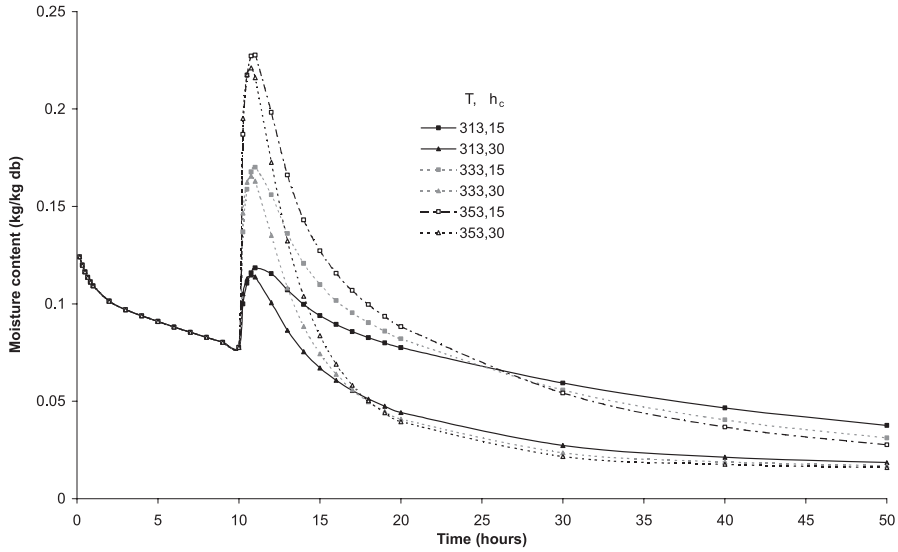


**Figure 14.**
Effect of $T$ and $h_c$ on evolution of moisture content at surface for $\phi$ = 70 per cent

the moisture evolutions for temperatures 333 and 353 K tend to coincide with those of 313 K at their corresponding heat transfer coefficient values. No condensation is observed for air at 313 K with a heat transfer coefficient value of 30 W/m K, as also observed in the rate of drying curves discussed earlier. The reduction in moisture content is faster for lower values of relative humidity. After any initial condensation, as the relative humidity increases, the difference in the quantity of moisture removal due to a change in heat transfer coefficient, increases.

## Conclusions

The drying model developed, based on the continuum approach, has been used to study the drying kinematics of a number of two stage drying regimes. A series of simulations of the drying behaviour of a rectangular brick with varying temperature, heat transfer coefficient and relative humidity of the drying medium have been undertaken. Based on these studies the following conclusions can be drawn.

- In general the total drying time is dependent on the relative humidity of the drying medium.
- The temperature and heat transfer coefficient affect the drying behaviour of the solid only during the initial transients of the second stage of drying.
- The condensation observed in the initial heating period of a second drying stage is related directly to increased relative humidity and temperature of the drying medium and lower heat transfer coefficients.

- During drying the solid reaches thermal equilibrium much faster than moisture equilibrium. The time taken to achieve thermal equilibrium is directly related temperature and inversely related to the heat transfer and relative humidity of the drying medium.
- Reduction in moisture content on the surface of the brick is faster for lower values of relative humidity. After any initial condensation, as the relative humidity increases, the difference in the quantity of moisture removal due to a change in heat transfer coefficient, increases.

Overall, it can be concluded that multistage drying regimes are useful in reducing the overall drying time. The use of the numerical solution considered here has allowed the effects of two stage drying of a two dimensional brick to be considered. In particular, the coupling between the moisture and thermal fields has been addressed and the resulting effects of varying drying conditions studied.

**References**

Comini, G., Lewis, R.W. (1976), "A numerical solution of two-dimensional problems involving heat and mass transfer", *Int. J. Heat Mass Transfer*, Vol. 19, pp. 1387–92.

Dietl, C., Winter, E.R.F. and Viskanta, R. (1998), "An efficient simulation of the heat and mass transfer processes during drying of capillary porous hygroscopic materials", *Int. J. Heat Mass Transfer*, Vol. 41, pp. 3611–25.

Ferguson, W.J. and Lewis, R.W. (1991), "A comparison of a fully non-linear and a partially non-linear heat and mass transfer analysis of a timber drying problem", *Proceedings of the VII International Conference on Numerical Methods in Thermal Problems*, Vol. VII, Part. 2, pp. 973–84.

Ford, R.W. (1986), *Ceramics Drying*, Pergamon Press, Oxford.

Fyhr, C. and Rasmuson, A. (1997), "Some aspects of modelling of wood chips drying in superheated steam", *Int. J. Heat Mass Transfer*, Vol. 40, pp. 2825–42.

Hawlader, M.N.A., Chou, S.K. and Chua, K.J. (1997), "Development of design charts for tunnel dryers", *Int. J. Energy Research*, Vol. 21, pp. 1023–37.

Huang, C.L.D. (1979), "Multi-phase moisture transfer in porous media subjected to temperature gradient", *Int. J. Heat Mass Transfer*, Vol. 22, pp. 1295–1307.

Kallel, F., Galanis, N., Perrin, B. and Javelas, R. (1993), "Effects of moisture on temperature during drying of consolidated porous materials", *J. Heat Transfer, ASME Trans.*, Vol. 115, pp. 724–33.

Kowalski, S.J., Musielak, G. and Rybicki, A. (1997), "The response of dried materials to drying conditions", *Int. J. Heat Mass Transfer*, Vol. 40, pp. 1217–26.

Luikov, A.V. (1996), *Heat and Mass Transfer in Capillary Porous Materials*, Pergamon Press, New York, NY.

Murugesan, K., Seetharamu, K.N. and Aswatha Narayana, P.A. (1996), "A one dimensional analysis of convective drying of porous materials", *Heat and Mass Transfer*, Vol. 32, pp. 81–8.

Murugesan, K., Seetharamu, K.N., Aswatha Narayana, P.A., Thomas, H.R. and Ferguson, W.J. (2000), "Study of shrinkage stresses for drying of brick as a conjugate problem", *Int. J. for Numerical Methods in Engineering*, Vol. 48, pp. 37–53.

Nasrallah, S.B. and Perre, P. (1988), "Detailed study of a model of heat and mass transfer during convective drying of porous media", *Int. J. Heat Mass Transfer*, Vol. 31, pp. 957–67.

Oliveira, L.S. and Haghighi, K. (1995), "Conjugate/adaptive finite element analysis of convective drying of porous media", *Proceedings of IX International Conference for Numerical Methods in Thermal Problems*, Vol. IX, pp. 80–8.

Perre, P., Turner, I.W. and Passard, J. (1999), "2-D solution of drying with internal vaporization of anisotropic media", *AIChE Journal*, Vol. 45, pp. 13–26.

Van Der Zanden, A.J.J. and Schoenmakers, A.M.E. (1996), "The influence of sorption isotherms on the drying of porous materials", *Int. J. Heat Mass Transfer*, Vol. 39, pp. 2319–27.